Annealing Accounts for the Length of Actin Filaments Formed by Spontaneous Polymerization

David Sept,* Jingyuan Xu,# Thomas D. Pollard,*§ and J. Andrew McCammon*

*Department of Chemistry and Biochemistry, University of California-San Diego, La Jolla, California 92093-0365; #Department of Biophysics and Biophysical Chemistry, The Johns Hopkins School of Medicine, Baltimore, Maryland 21205; and §Salk Institute for Biological Studies, La Jolla, California 92037 USA

ABSTRACT We measured the lengths of actin filaments formed by spontaneous polymerization of highly purified actin monomers by fluorescence microscopy after labeling with rhodamine-phalloidin. The length distributions are exponential with a mean of ~7 μm (2600 subunits). This length is independent of the initial concentration of actin monomer, an observation inconsistent with a simple nucleation-elongation mechanism. However, with the addition of physically reasonable rates of filament annealing and fragmenting, a nucleation-elongation mechanism can reproduce the observed average length of filaments in two types of experiments: 1) filaments formed from a wide range of highly purified actin monomer concentrations, and 2) filaments formed from 24 μM actin over a range of CapZ concentrations.

INTRODUCTION

Actin polymerization is important not only for cellular structure and function, but also as a model system for studies of macromolecular self-assembly. The goal of this work is a complete quantitative model to use as the starting point for evaluating the effects of actin-binding proteins on polymerization in cells. The pioneering work of Oosawa and Asakura (1975) established that spontaneous polymerization of actin monomers requires an unfavorable nucleation step followed by rapid elongation. Elongation is more accessible experimentally than nucleation, so it is much better understood, with a complete set of rate constants for association and dissociation of ATP-actin and ADP-actin subunits at both ends of the filament (Pollard, 1986 and references therein). Nucleation has been studied by observing the complete time course of spontaneous polymerization as a function of actin monomer concentration and then finding a set of reactions and rate constants that fit these kinetic data (Tobacman and Korn, 1983; Cooper et al., 1983; Frieden, 1983; Frieden and Goddette, 1983). These studies concluded that actin dimers are less stable than trimers, which are the nucleus for elongation. Under the usual experimental conditions, the concentrations of dimers and trimers are very low, owing to their instability and the rapid consumption of trimers by elongation. This approach puts relatively loose constraints on the values of the rate and equilibrium constants for the nucleation reactions.

In addition to nucleation and elongation, Oosawa and Asakura established that actin filaments can break and anneal end-to-end. Inclusion of a fragmentation reaction improved the fit of nucleation-elongation mechanisms to the observed time course of polymerization under some conditions (Wegner and Savko, 1982; Cooper et al., 1983; Buzan and Frieden, 1996) and the presence of tropomyosin appears to inhibit fragmentation during polymerization (Wegner, 1982; Hitchcock-DeGregori et al., 1988). For annealing, there has been kinetic evidence both for (Kinosian et al., 1993; Rickard and Sheterline, 1988) and against (Carlier et al., 1984) its role in length redistribution after sonication, but the most direct evidence from electron micrographs supports rapid annealing (Murphy et al., 1988). Nevertheless, the contribution of fragmentation and annealing to the products of spontaneous polymerization is not well-established because the previous experimental data did not constrain the mechanisms well enough to assess the importance of these reactions.

We used improved light microscopic methods (Burlacu et al., 1992) to repeat classic experiments of Kawamura and Maruyama (1969, 1972) on the length of actin filaments, obtaining completely different results that are incompatible with a simple nucleation-elongation mechanism of spontaneous polymerization. The observed filaments are longer than expected and the lengths are independent of the starting actin monomer concentration. These new data gave us the opportunity to use modeling to quantitatively assess the contribution of annealing and fragmentation to spontaneous polymerization. A new, physically reasonable model of polymerization, including annealing and fragmentation reactions, accounts for the observed lengths of actin filaments over a wide range of actin monomers.

Received for publication 16 April 1999 and in final form 19 August 1999.

Address reprint requests to Dr. David Sept, Department of Chemistry and Biochemistry, 0365, University of California-San Diego, 9500 Gilman Drive, La Jolla, CA 92093-0365. Tel.: 619-534-2913; Fax: 619-534-7042; E-mail: dsept@ucsd.edu.

0006-3495/99/12/2911/09 $2.00

MATERIALS AND METHODS

Solutions

Buffer G contained 0.2 mM ATP, 0.5 mM dithiothreitol, 0.1 mM $CaCl_2$, 1 mM sodium azide, and 2 mM Tris-Cl, pH 8.0, at 25°C. Concentrated polymerizing buffer (10xKME) contained 500 mM KCl, 10 mM $MgCl_2$, 10 mM EGTA, and 20 mM Tris-Cl, pH 8.0 or 100 mM imidazole pH 7.0, at 25°C. A fluorescence microscopy buffer modified from Kron et al. (1991)

contained 50 mM KCl, 1 mM $MgCl_2$, 100 mM dithiothreitol, 20 μg/ml catalase, 0.1 mg/ml glucose oxidase, 3 mg/ml glucose, and 2 mM Tris-Cl, pH 8.0, or 10 mM imidazole, pH 7.0, at 25°C.

Protein purification

Actin was prepared from rabbit skeletal muscle by extraction from acetone powder, a cycle of polymerization, pelleting, and depolymerization, followed by gel filtration on a 2.5 × 110 cm column of Sephacryl S-300 equilibrated with Buffer G (MacLean-Fletcher and Pollard, 1980). The peak and following 4-ml fractions were pooled, stored in continuous dialysis with daily changes of fresh buffer G, and used for experiments within five days. Some actin was purified further to remove CapZ (Casella et al., 1995). The fractions beginning at the midpoint of the leading edge of the actin peak of the first gel filtration column were pooled and repolymerized with 50 mM KCl and 2 mM $MgCl_2$. The pelleting, depolymerization, and gel filtration steps were repeated.

Measurement of actin filament lengths

Because the samples need to be diluted well below the critical concentration for fluorescence microscopy, we stabilized them with CapZ (which blocks the rapidly depolymerizing barbed end without severing the filaments) and with rhodamine-phalloidin (which not only labels filaments with rhodamine, but also reduces subunit dissociation at both ends to near zero (Coluccio and Tilney, 1984; Sampath and Pollard, 1991). Fixation with aldehydes was considered, but rejected because they are known to damage actin filaments (Lehrer, 1972). To minimize shearing and artifactual fragmentation of filaments during manipulations, we trimmed the tip of the plastic pipette tip (Burlacu et al., 1992; Janmey et al., 1994).

Actin was polymerized by adding one part of the concentrated polymerizing buffer 10xKME to nine parts of actin in Buffer G. After 3 h incubation, we added one CapZ per 500 actin subunits and one rhodamine-phalloidin (Molecular Probes, Eugene, OR) per actin subunit and diluted the sample to 0.3 μM with fluorescence buffer (Burlacu et al., 1992; Kaufmann et al., 1992; Käs et al., 1996). After incubation at room temperature for 30 min to allow rhodamine-phalloidin binding (De La Cruz and Pollard, 1994), the labeled actin was diluted to 2–10 nM with fluorescence buffer, ~10 μl of solution was placed on a microscope slide and covered with a 20-mm-square coverslip coated with nitrocellulose. After several minutes all of the filaments that we could detect by fluorescence microscopy attached to the coverslip, leaving no filaments free in the solution in the 25 μm gap between slide and coverslip. Filaments were observed with a Leitz Orthoplan microscope equipped with a 3-mm BG-38, KP 560 (short wavelength pass interference filter), 2-mm BG-36 (excitation filter), TK-580 (dichroic mirror), two K-580 (colored glass barrier filters), and an Olympus 100× (NA 1.25) objective. Images were recorded on Kodak 3200 black-and-white professional film with an exposure of 30–60 s. The image quality of the photos (Fig. 1) was superior to those acquired with a Hamamatsu Vidicon Video Camera C1000. Images of the filaments were clear enough to measure filament lengths >0.3 μm manually on prints at a final magnification of 3150×. Small fluorescent spots due to filaments <0.3 μm were grouped together in a category of 0–0.5 μm. The short filaments appeared as fluorescent spots rather than asymmetrical filaments. Negative films were digitized with Adobe Photoshop 3.0. Taking a filament >2 μm long as the internal standard for fluorescence per unit length, we used National Institutes of Health Image 1.6 to evaluate the lengths of each fluorescent spot in the whole population of short filaments on the same negative. A blank area was used to measure the background to subtract from the areas containing each fluorescent filament. The number average length (L_n) is defined as $L_n = (1/n)\Sigma l_i$, where n is the number of filaments and l_i is the length of each filament. The length distributions were approximately exponential rather than Gaussian, so standard deviation could not be used to describe the variability. For an exponential distribution, the fraction of filaments (f_i) with length l is $f_i = \lambda\exp(-\lambda l_i)$, the mean length is $1/\lambda$, and the variance $(l_i) = (1/\lambda)^2$.

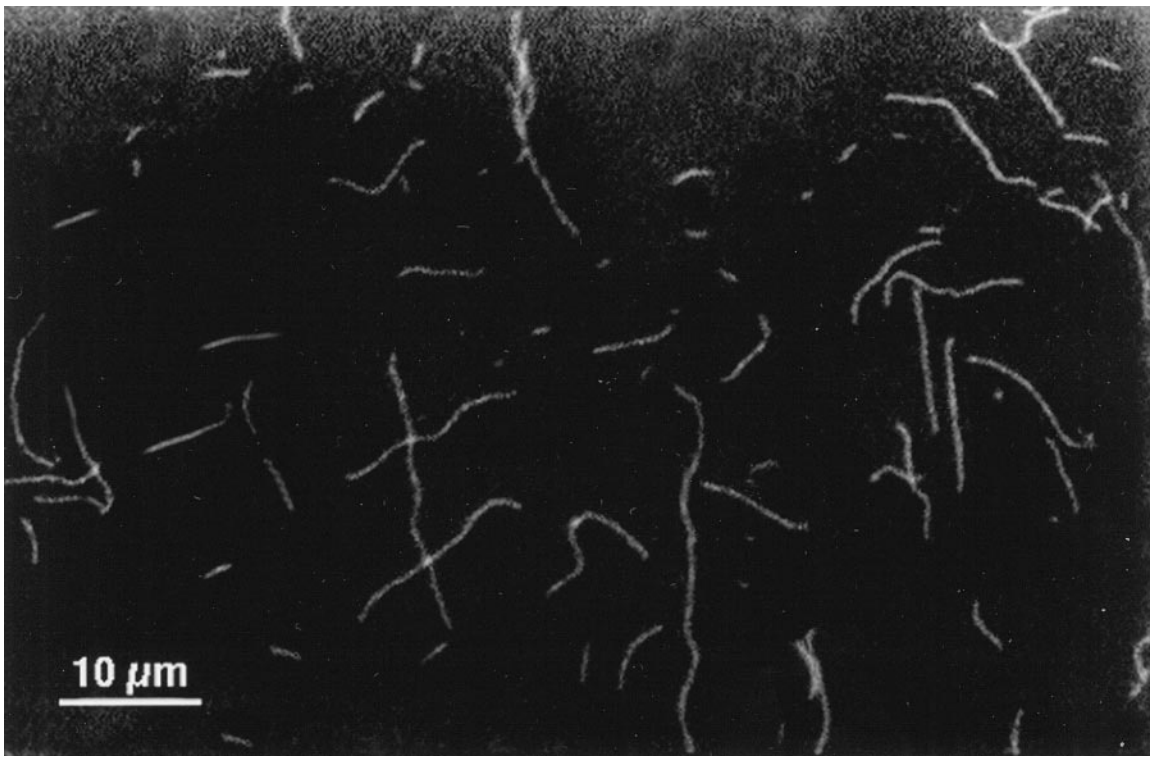

FIGURE 1 Fluorescence micrographs of actin filaments labeled with rhodamine-phalloidin for singly gel-filtered actin. Conditions: 24 μM actin, 50 mM KCl, 1 mM $MgCl_2$, 1 mM EGTA, 180 μM ATP, 0.45 mM DTT, 90 μM $CaCl_2$, 0.9 mM azide, 4 mM Tris-Cl (pH 8.0), 22°C for 3 h.

RESULTS

Actin filament lengths

We measured actin filament lengths by fluorescence microscopy after labeling with rhodamine-phalloidin. All detectable filaments in the samples attached to the nitrocellulose-coated glass, so we assume that the length distribution of filaments on the coverslip reflects the distribution in solution. As filaments in solution bound to the nitrocellulose coating the coverslip, ~10%, especially longer ones, broke. For example, in a sample of 60 filaments five broke while approaching the coverslip surface: two filaments broke into two pieces, two into three, and one into four. Thus, the sample on the coverslip slightly underestimates the distribution of lengths in solution. The method may also miss some filaments <0.2 μm long due to their faint fluorescence. For comparison, we coated coverslips with rabbit skeletal muscle myosin treated with N-ethylmaleimide to inhibit the ATPase activity but not actin binding (Warshaw et al., 1990). The filaments bound to myosin had the same length distribution and number average length as filaments on nitrocellulose.

We measured lengths >0.5 μm directly, but used densitometry for samples consisting primarily of filaments <2 μm long. When two observers measured the same sample, they recorded the same length distribution and number average length. The length distributions and average lengths did not change between 3 h and two days after polymerization, so we concluded that 3 h is sufficient to reach a steady state. Actin filament length distributions and average lengths were the same in polymerization buffer at pH 8.0 and pH 7.0.

Filaments assembled by spontaneous polymerization from doubly gel-filtered actin monomers at 24 μM varied in length from <0.3 μm to several tens of micrometers (Figs. 1 and 2 *A*). We observed many filaments over 10 μm long, one close to 100 μm. The distribution of lengths was exponential and the mean length was 6.7 μm. The number average length was remarkably independent of the concentration of pure monomers used to assemble the filaments (Fig. 3).

The filament length distribution depended on the purity of the actin monomers (Figs. 2 and 3). Before a second cycle of polymerization, depolymerization and gel filtration to remove traces of capping protein (Casella et al., 1995), the filaments were ~20% shorter and the length distribution was more uniform. This confirms the prediction (Casella et al., 1995) that the low concentration of CapZ in singly gel-filtered actin slightly reduces the length of actin filaments. This is true even though we used only the fractions from the top of the actin monomer peak to avoid CapZ, the peak of which chromatographs ahead of actin monomers. In contrast to doubly gel-filtered actin, the number average length of singly gel-filtered actin increased slightly with starting actin concentration (Fig. 3).

Description of the model

The basis of the standard nucleation-elongation model is one or more unfavorable nucleation steps followed by more favorable elongation (Oosawa and Asakura, 1975). Previous models for actin polymerization showed that the critical size for the nucleus is somewhere between a dimer and a trimer, and that the number of explicit nucleation steps does not affect the results of the model (Tobacman and Korn, 1983; Cooper et al., 1983; Frieden, 1983; Frieden and Goddette, 1983). We also found that choosing a critical nucleus larger than three or four monomers did not affect the results of the model. With these considerations in mind, we propose a

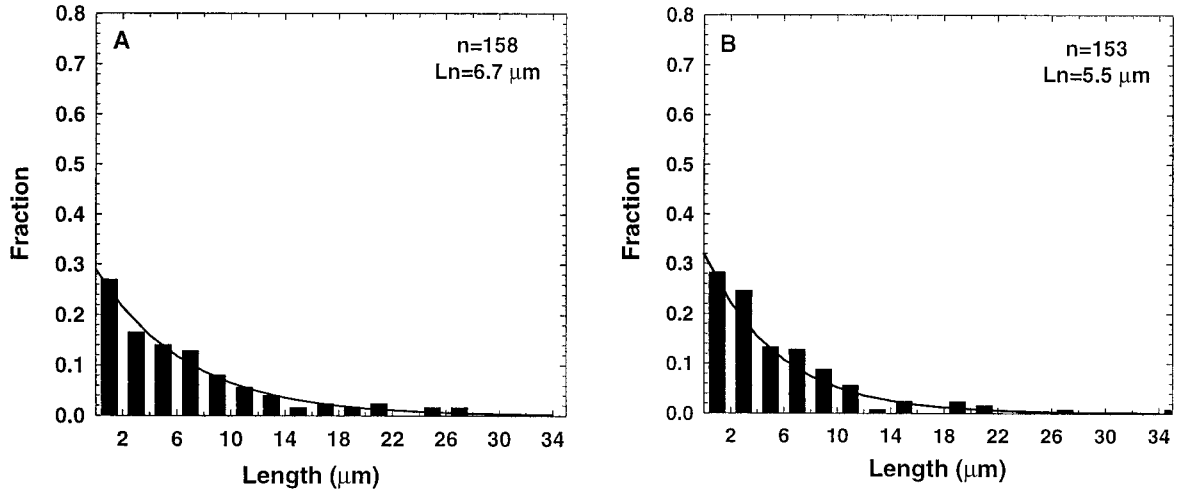

FIGURE 2 Length distributions of actin filaments. Lines in (*A*) and (*B*) are exponentials. Conditions as in Fig. 1. (*A*) Doubly gel-filtered actin. (*B*) Singly gel-filtered actin.

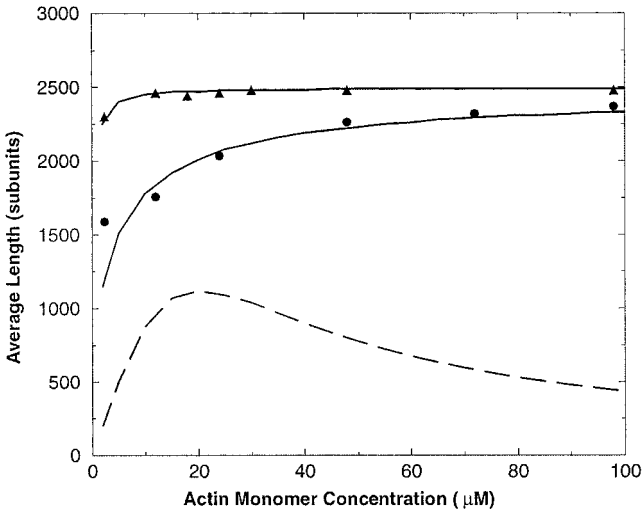

FIGURE 3 Dependence of the number average length (L_n) of actin filaments on the purity and monomer concentration during polymerization. Conditions as in Fig. 1, except that the actin monomer concentration during polymerization was varied as indicated. The filaments formed during each 30-ms interval were allowed to elongate over the succeeding course of the reaction. (●), Singly gel-filtered actin; (▲), doubly gel-filtered actin. Theoretical lengths calculated by kinetic simulation using the nucleation-elongation model and the rate constants in the text without annealing/fragmenting (*dashed line*) and with both annealing and fragmenting (*solid line*).

simple five-step model

$$A + A \underset{k_{-1}}{\overset{k_{+1}}{\rightleftharpoons}} A_2 \qquad k_{+1} = 10\ \mu\mathrm{M}^{-1}\,\mathrm{s}^{-1} \quad k_{-1} = 10^6\ \mathrm{s}^{-1}$$

$$A + A_2 \underset{k_{-2}}{\overset{k_{+2}}{\rightleftharpoons}} A_3 \qquad k_{+2} = 10\ \mu\mathrm{M}^{-1}\,\mathrm{s}^{-1} \quad k_{-2} = 10^3\ \mathrm{s}^{-1}$$

$$A + A_3 \underset{k_{-3}}{\overset{k_{+3}}{\rightleftharpoons}} A_4 \qquad k_{+3} = 10\ \mu\mathrm{M}^{-1}\,\mathrm{s}^{-1} \quad k_{-3} = 10\ \mathrm{s}^{-1}$$

$$A + A_4 \underset{k_{-4}}{\overset{k_{+4}}{\rightleftharpoons}} N \qquad k_{+4} = 10\ \mu\mathrm{M}^{-1}\,\mathrm{s}^{-1} \quad k_{-4} = 0\ \mathrm{s}^{-1}$$

$$A + N \underset{k_{-}}{\overset{k_{+}}{\rightleftharpoons}} N \qquad k_{+} = 10\ \mu\mathrm{M}^{-1}\,\mathrm{s}^{-1} \quad k_{-} = 1\ \mathrm{s}^{-1} \qquad (1)$$

We use A to represent the concentration of actin monomers, A_i for a filament with i actin monomers, and N represents the concentration of all longer filaments. The rate constants for the last reaction are experimentally measured (Pollard, 1986) and lead to the correct critical concentration ($C_c > 0.1\ \mu$M), but the other rate constants are only approximations from kinetic simulations, chosen to reproduce the time course of polymerization over a limited range of actin monomer concentrations. Such polymerization curves have already been published by other investigators (Wegner and Savko, 1982; Tobacman and Korn, 1983; Cooper et al., 1983; Frieden, 1983; Frieden and Goddette, 1983; Buzan and Frieden, 1996). Filaments longer than four subunits are assumed to be stable and the back-reaction rate k_{-4} is set to zero. This is appropriate because most filaments are much longer than four monomers. The coupled first-order differential equations that arise from the set of reactions in Eq. 1 are "stiff-equations" due to the large differences in the forward and back reaction rates. Because of this, we used a semi-implicit scheme to solve the system of equations (Press et al., 1992). This set of equations produces correct polymerization curves, but the average length as a function of actin concentration is completely incorrect. The mean lengths of the observed filaments are almost independent of the initial concentration of actin monomers, while this simple model predicts a mean length with quite a different behavior, especially at high concentrations of actin (see Fig. 3). To solve this problem we must consider additional processes in our model.

Expanding the basic model

The average length is simply given by the total amount of polymer divided by the total number of filaments formed. Inasmuch as Eq. 1 produces the correct time course and extent of polymerization but not the correct average length, the simple model produces the incorrect number of filaments. The average length is too low, so the actual mechanism must produce fewer filaments. We can represent the number of filaments in our system as the number of filaments that are formed by the addition of a monomer onto a polymer A_4. Because there is no back-reaction rate for this process, the equation for the change in N, the filament number concentration, is simply

$$\dot{N} = k_+ A A_4 \qquad (2)$$

Addition of monomers to existing filaments increases the concentration of polymerized actin, but does not increase N. If we want to include filament annealing, we should also consider the breakup of a filament or fragmentation. To include filament annealing and fragmenting in our reaction scheme, we can add the following reaction

$$N + N \underset{k_f}{\overset{k_a}{\rightleftharpoons}} N \qquad (3)$$

where k_a represents the annealing rate and k_f the fragmentation rate of a filament. Because two filaments are joined to form a new filament the annealing rate has a quadratic dependence and our new equation for the change in N is

$$\dot{N} = k_+ A A_4 - k_a N^2 + k_f N \qquad (4)$$

To choose values for k_a and k_f we need to consider several things. The addition of a monomer to the fast-growing barbed end of a filament is a diffusion-limited process, so it is reasonable to assume that annealing of two filaments is also limited by diffusion, as similar bonds are formed and filaments diffuse more slowly than monomers. Murphy et al. (1988) performed ultrasonification experiments to esti-

mate the rate of annealing. Following sonification they found an initial rate constant for annealing of $k_a = 10\ \mu M^{-1}\ s^{-1}$ for very short filaments, but as annealing progressed and the filaments became longer, the rate fell off rapidly with time. Kinosian et al. (1993) were also able to measure the rate of annealing after sonication and found a rate of 2.2 $\mu M^{-1}\ s^{-1}$. If k_a is diffusion-limited, the diffusion that we need to consider is the relative diffusion of the two filaments. It is difficult to write an accurate expression for the movement of an individual polymer embedded in a polymer gel. The most common treatment uses the reptation idea (de Gennes, 1990; Doi and Edwards, 1987). In fact, actin filaments at high enough concentration (above 40 nM filament concentration) have been shown to exhibit reptation motion (Janmey et al., 1994; Käs et al., 1996). The transverse diffusion is controlled by the mass of the polymer and the density of the polymer network, but the diffusion constant along the tube is inversely proportional to the length of the filament (Käs et al., 1996) having the form

$$D_{\parallel} = \frac{k_B T}{\zeta L} \tag{5}$$

where ζ is the friction coefficient. We choose the annealing rate constant k_a to be proportional to $D_{\parallel}$, namely

$$k_a = k_a'/L \tag{6}$$

where all of the constants are absorbed in the variable k_a'.

Erickson (1989) previously estimated the fragmentation rate to be in the neighborhood of $k_f \approx 10^{-8}\ s^{-1}$. The rate is very low because it involves breaking more than one bond in the filament, but as it is equally probable between any given pair of monomers, the rate should be proportional to the length of the filament. The gel network that is formed may also affect the amount of fragmentation. Within the gel, each individual filament is constrained by its neighbors or, in reptation terms, by the filaments that make up the reptation tube. Doi (1975) showed that the number of rods within a distance b of a given rod is given by bL^2N, where L is the filament length and N is still the filament concentration. If we choose an additional fragmentation rate proportional to this quantity, we can write

$$k_f = k_{f1}'L + k_{f2}'L^2N \tag{7}$$

where once again we absorbed all the constants into the two factors k_{f1}' and k_{f2}'. It is not readily apparent how the polymer gel will affect filament fragmentation: will the network that is formed tend to strain the filaments and increase breakage, or will the confinement within the reptation tube tend to decrease the amount of fragmentation? To answer this question, the constant k_{f2}' will be treated as a free parameter in a minimization scheme, and the sign of k_{f2}' resulting best fit will determine whether this leads to an increase or decrease in k_f.

If we replace k_a and k_f in Eq. 4 we get

$$\dot{N} = k_+AA_4 - k_a'\frac{N^2}{L} + k_{f1}'LN + k_{f2}'L^2N^2 \tag{8}$$

The amount of polymerized protein in our system is given by the expression

$$P = A_0 - A - 2A_2 - 3A_3 - 4A_4 \tag{9}$$

where A_0 represents the initial actin concentration. Using this expression, the average length of a filament is given simply by $L = P/N$. If we make this replacement for L, we get

$$\dot{N} = k_+AA_4 - k_a'\frac{N^3}{P} + k_{f1}'P + k_{f2}'P^2 \tag{10}$$

Note that as the actin concentration is increased and more protein polymerizes, the rate of annealing decreases while the fragmentation rate increases. The values for the rate constants depend on the actin concentration and the filament density and length.

When actin is purified from cells such as skeletal muscle, some actin-associated proteins remain in the sample, including the capping protein CapZ. We can include a reaction for capping filaments. This reaction can be written

$$\text{CapZ} + N \underset{k_{z-}}{\overset{k_{z+}}{\rightleftharpoons}} N^* \tag{11}$$

where N^* now represents a filament that is capped at the barbed end, preventing monomer addition or dissociation and annealing. The constants for the above reaction are $k_{z+} \approx 3.5\ \mu M^{-1}\ s^{-1}$ and $k_{z-} \approx 3 \times 10^{-4}\ s^{-1}$ (Schafer et al., 1996). With this added reaction, the total number of filaments in our system is $N + N^*$ and the average length is now given by

$$L = \frac{P}{N + N^*} \tag{12}$$

A capped filament can still fragment, but a capped filament can only anneal with an uncapped filament, because this requires at least one free barbed end. Inasmuch as two uncapped filaments can anneal in two ways, but capped and uncapped filaments have only one method of annealing, the rate of annealing is half the original value. With these additions, the equations for the change in N and N^* become

$$\dot{N} = k_+AA_4 - k_a'\frac{N(N + \frac{1}{2}N^*)}{L} + k_{f1}'P + k_{f2}'P^2 - k_{z+}N + k_{z-}N^* \tag{13}$$

$$\dot{N}^* = k_{z+}N - k_{z-}N^* \tag{14}$$

where L is given by Eq. 12.

To find the mean length predicted by our model, we must solve Eqs. 1, 13, and 14 for a given initial actin monomer concentration A_0 and then calculate the average length using Eq. 12. During the polymerization of actin monomers, the rates for annealing and fragmentation will change with time because they depend on the filament length and density. The rate of annealing immediately following sonication has been

measured in the range 2.2–10 $\mu M^{-1}\ s^{-1}$ (Kinosian et al., 1993; Murphy et al., 1988). Because $k_a = k'_a/L$ and $L \simeq 30$ (subunits) following sonication, we chose $k'_a = 300\ \mu M^{-1}\ s^{-1}$ so that $k_a = 10\ \mu M^{-1}\ s^{-1}$ for $L = 30$. The factors k'_{f1} and k'_{f2} were treated as free parameters for fitting the two curves for mean polymer length versus actin concentration for singly and doubly filtered actin. The rate constants for the nucleation-elongation steps (Eq. 1) were fixed at the values previously used to reproduce polymerization curves. We developed a procedure to minimize the RMS difference between the experimental and theoretical results by changing the constants k'_{f1} and k'_{f2}. We could not fit both curves with the same values for k'_{f1} and k'_{f2}, but required a larger value of k'_{f1} for the singly filtered actin. One possible explanation for this is the presence of other actin-associated proteins in the singly filtered sample. We estimate that singly filtered actin contains about one part in 50,000 CapZ, and other proteins, such as severing proteins, could also be present at higher concentration in the singly gel-filtered than doubly gel-filtered actin. These latter proteins cut actin filaments, and because they act with equal probability along the length of a filament, the severing rate is proportional to L. Thus, the presence of low concentrations of severing proteins results in a larger value for k'_{f1} for singly filtered actin. It is also possible that the CapZ that is present in the singly filtered actin in some way increases the fragmentation rate, perhaps by changing the structure of a filament upon when it binds. With these points in mind, we chose a fixed value of k'_{f2} and two different values of k'_{f1}, a higher value for the singly filtered than doubly filtered actin. The values chosen were $k'_{f2} = 1.8 \times 10^{-8}\ \mu M^{-1}\ s^{-1}$, and $k'_{f1} = 2.0 \times 10^{-7}\ s^{-1}$ and $1.1 \times 10^{-8}\ s^{-1}$ for the singly and doubly gel-filtered actin, respectively. The value of k_a will change as the average filament length increases. To compare this behavior with experimental measurements we performed a "sonication simulation." For this simulation we allowed the system to reach equilibrium and then manually set the average filament length equal to 30 (P remained untouched while N was adjusted so that $L = 30$). In agreement with the experimental observations of Murphy et al. (1988), the annealing rate constant falls off rapidly with time following sonication (see Fig. 4). For k_f, the term with k'_{f1} only contributes ~2% toward the value of k_f in the doubly filtered actin. In the singly filtered case, perhaps due to the presence of other severing proteins, k'_{f1} and k'_{f2} contribute roughly equally to the fragmentation rate.

This model including annealing and fragmentation agrees with the observed lengths over a wide range of starting actin monomer concentrations (Fig. 3). In these calculations we assumed that the ratio of CapZ to actin in the singly filtered actin is ~1:50,000, and zero in the doubly filtered actin. Note that a 1:50,000 concentration ratio corresponds to about one CapZ molecule for every 20 filaments. It is interesting to see the influence such a small amount of CapZ has on the average filament length. This effect was predicted by Casella et al. (1995).

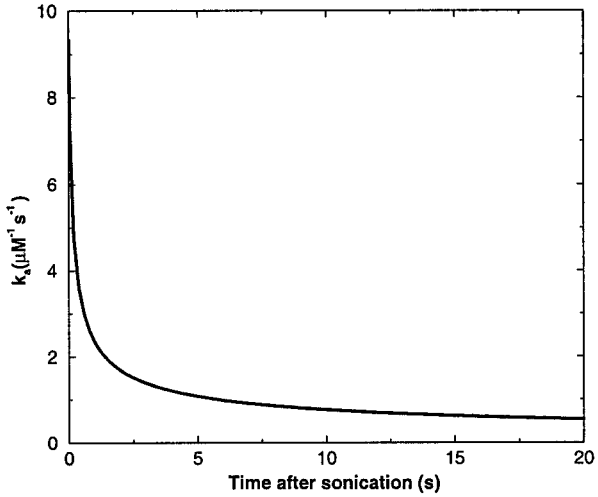

FIGURE 4 The rate of annealing (k_a in Eq. 6) as a function of time in a sonication simulation. This represents the solution of Eqs. 1, 13, and 14 with an initial actin monomer concentration of 24 μM. The system was allowed to reach equilibrium at which point the filament concentration N was manually set so that the average length L was equal to 30 subunits, a value consistent with what is observed in sonication experiments, and the system was again allowed to equilibrate.

The minor disagreement between the theory and experiment at low actin concentration may be due to the breakdown of the reptation idea at low concentrations. When the concentration is low enough and the system is in the "dilute" regime, the actual diffusion constant is larger because a filament is not constrained to move within a tube. This results in more annealing, fewer filaments, and a longer average length. The crossover from the dilute to reptation region occurs at an actin concentration of ~25 μM. At this concentration the filament number concentration in the simulations is ~30 nM, close to the 40 nM found in experiment (Käs et al., 1996). Above 25 μM, where reptation should occur, there appears to be good agreement between experiment and our model.

Apart from looking at the effect of actin concentration on the average length, we can reverse the situation by fixing the actin concentration and varying the amount of CapZ. This provides a direct test of both the rate constants we fixed by fitting the first data sets and the effect of CapZ within our model. Nanomolar concentrations of CapZ are required for a dramatic effect on the mean length (Fig. 5) and above ~10 nM, all of the filaments are expected to be capped. Again the results of our model agree well with experimental observations (Xu et al., 1999).

DISCUSSION

Experimentalists have struggled to reach a consensus on the length distributions of actin filaments polymerized in vitro. Light microscopy of filaments labeled with rhodamine-phalloidin appears to be the most reliable method for measuring lengths, although we observed that a few filaments break during adsorption to the coverslip. Electron micros-

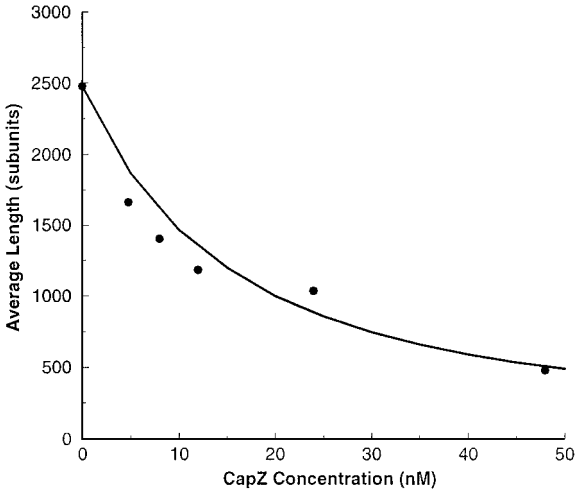

FIGURE 5 The average length of actin filaments as a function of CapZ concentration as predicted by our theory and measured by experiment (data taken from Xu et al., 1999). The actin monomer concentration in both cases is 24 μM and the rate constants for the simulation are the same as the doubly filtered actin plot in Fig. 3.

copy appears to underestimate lengths even more. However, results differ even with light microscopy. We find that filaments of highly purified actin have an exponential distribution of lengths with a mean of ~2500 subunits. We have no direct standard of comparison, because all previous work used actin contaminated with capping proteins. Our measurements with once-cycled actin containing about one CapZ per 10,000 actins agree in general with the light microscopic results of Burlacu et al. (1992), but not with others. Kaufmann et al. (1992) and Käs et al. (1996) reported mean lengths around 20 μm (7400 subunits) with a broad and irregular distribution of lengths. One figure in Käs et al. (1996) had an exponential distribution of lengths with an average length of 4.6 μm, similar to our observations. Short filaments are difficult to detect, particularly in solution. Omission of some short filaments would give mean lengths greater than the true mean length.

Simple nucleation-elongation theories can describe the time course and extent of many polymerizing systems, including the self-assembly of actin. However, these polymerization models have not been constrained to fit measured polymer lengths. We show here that additional reactions, especially end-to-end annealing of filaments, are required to account for the observed lengths. Ignoring annealing was reasonable in earlier work, where the emphasis was on fitting polymerization curves. Even in this extended model, the inclusion of annealing has a very minimal effect on the simulated time course of polymerization, changing the half-time of polymerization by <1%. Annealing changes the number of filaments but not the concentration of polymer. This is most easily seen in the fact that k_a and k_f do not appear in Eq. 1, and that the total amount of polymerization, P, is solely determined by the four quantities A_i in Eq. 1. Elongation is fast, with a maximum rate at the outset of polymerization, while annealing is slow, increasing in importance as the polymerization steps in Eq. 1 reach their equilibrium.

Our improved model for actin polymerization extends the simple nucleation-elongation mechanism (Eq. 1) to include annealing and fragmentation of actin filaments and the effects of contaminating proteins. The underlying premise of this mechanism is several unfavorable nucleation steps followed by more favorable elongation once a stable nucleus is achieved. Nucleation and elongation steps are directly affected by the actin monomer concentration, while the additional processes depend on the length and concentration of the actin filaments. Annealing is a diffusion-limited process and the diffusion constant for a filament is inversely proportional to its length (Käs et al., 1996). The annealing rate constant is initially $\sim 10\ \mu M^{-1}\ s^{-1}$ (following sonication) when most of the filaments are short, but rapidly falls off with time for two reasons. First, the annealing rate constant is an inverse function of the mean length, which increases with time. Second, annealing is a second-order reaction that requires the interaction of two filaments, and the filament number decreases with time. The initial value and time behavior of the rate constant are in agreement with experimental observations (Murphy et al., 1988).

Two different processes contribute to fragmentation. The first reaction rate is proportional to the length of the filament. This represents both the unfavorable breaking of an actin filament at some point along its length and the severing of a filament by actin-associated proteins such as gelsolin. The second contribution, proportional to the filament concentration and the square of the filament length, is due to the number of contacts between a given filament and its neighbors. As determined by fitting our model to the experimental data, these contacts should lead to an increase in fragmentation.

The values of the two fragmentation rate constants were treated as free parameters to fit the experimental data. Normally, the fragmentation process is written as $k_f P$, so it is proportional to the total amount of polymerized protein P. If we rewrite the fragmentation part of Eq. 13 as $(k'_{f1} + k'_{f2}P)P$, we can more easily compare our predicted rates with those from experiment. For a polymer concentration of 24 μM, we find that $(k'_{f1} + k'_{f2}P) = 4-6 \times 10^{-7}\ s^{-1}$ for singly and doubly filtered actin. These values are slightly higher than Erickson's theoretical value of $10^{-8}\ s^{-1}$ (Erickson, 1989), but are in agreement with the value measured by Kinosian et al. (1993) of $7 \times 10^{-7}\ s^{-1}$. The inclusion of severing proteins or increased fragmentation due to CapZ, even in low concentrations, is required to explain the difference between the singly and doubly gel-filtered actin, while fragmentation due to stress within the network is needed to counteract the elevated rate of annealing at high monomer concentrations. At present, there are no experimental data to directly compare with these rate constants, although the overall fragmentation rate appears to be reasonable.

The final consideration was the effect of capping protein, CapZ. Residual CapZ and other actin-associated proteins help explain the differences observed between singly and doubly gel-filtered actin. Capping a filament eliminates annealing at the barbed end, but does not affect the rate of fragmentation. The effect of contaminating CapZ was evaluated by adding CapZ to pure actin. Results (Fig. 5) provide experimental support for the rate constants and the effect of CapZ on annealing (Xu et al., 1999).

The addition of annealing and fragmenting causes a negligible change in the time course of polymerization, but primarily affects the concentration of filaments, and hence, the average length. At any given monomer concentration, a balance must be reached between annealing, which favors longer filaments, and fragmentation, which favors shorter ones. This balance appears to result in a mean length that, apart from the effect of CapZ and other proteins, is largely independent of the monomer concentration. It should be noted that the additional processes considered in this paper do not simply represent the addition of arbitrary steps to the polymerization process, but are physically realistic, experimentally observed phenomena. Furthermore, our study indicates that these additional steps represent a minimal extension to the standard nucleation-elongation theory needed to explain the time course of polymerization *and* the mean length observations.

Our theoretical model differs from experiment at low actin concentration where our assumption of reptation motion is no longer valid. Unfortunately, this crossover region from a semi-dilute to a dilute solution is difficult to characterize and model accurately. Future work may be able to solve this problem with a more accurate description of filament diffusion at lower actin concentrations. At the other end of the spectrum, namely high actin concentrations, nematic regions appear in the solution (Käs et al., 1996; Buxbaum et al., 1987; Suzuki et al., 1991; Coppin and Leavis, 1992; Furukawa et al., 1993). Within these domains filaments do not exhibit reptation, and the diffusion constant becomes almost independent of length. Also, because the filaments are no longer entangled, the rate of fragmenting due to contacts within the gel should decrease. In our model, both these factors would result in longer filaments in nematic domains as opposed to gel regions. Thus, as observed in vivo (Lewis and Bridgman, 1992), actin filaments should tend to be longer in bundles than in random networks. Our current model calculates the mean filament lengths but not length distributions. If the filaments were separated into bins according to their length in order to get these distributions, we could still handle polymerization, but the annealing and fragmentation processes would become extremely complicated, e.g., a filament of a given length could be formed by annealing any combination of two shorter filaments. Because our model already provides an adequate fit to experimental results, this added complication seems unnecessary.

We thank Paul Janmey and Julie Theriot for referring us to some important papers. J.X. is grateful to Xing Cao for help with calculations and to Jia Lu for the independent measurements of the filament lengths.

This work was supported by National Institutes of Health grants (to T.D.P. and J.A.M.), an NSERC fellowship awarded to D.S., and a Thomas C. Jenkins Fellowship given to J.X.

REFERENCES

Burlacu, S., P. A. Janmey, and J. Borjedo. 1992. Distribution of actin filament lengths measured by fluorescence microscopy. *Am. J. Physiol*. 262:C569–C577.

Buxbaum, R., T. Dennerll, S. Weiss, and S. Heidemann. 1987. F-actin and microtubule suspensions as indeterminate fluids. *Science*. 235: 1511–1514.

Buzan, J. M., and C. Frieden. 1996. Yeast actin: polymerization kinetic studies of wild type and a poorly polymerizing mutant. *Proc. Natl. Acad. Sci. USA*. 93:91–95.

Carlier, M. F., D. Pantaloni, and E. D. Korn. 1984. Steady state length distribution of F-actin under controlled fragmentation and mechanism of length redistribution following fragmentation. *J. Biol. Chem.* 259: 9987–9991.

Casella, J. F., E. A. Barron-Casella, and M. A. Torres. 1995. Quantitation of CapZ in conventional actin preparations and methods for further purification of actin. *Cell Motil. Cytoskeleton.* 30:164–170.

Coluccio, L. M., and L. G. Tilney. 1984. Phalloidin enhances actin assembly by preventing monomer dissociation. *J. Cell Biol*. 99:529–535.

Cooper, J. A., E. L. Buhle, Jr., S. B. Walker, T. Y. Tsong, and T. D. Pollard. 1983. Kinetic evidence for a monomer activation step in actin polymerization. *Biochemistry*. 22:2193–2202.

Coppin, C., and P. Leavis. 1992. Quantisation of liquid-crystalline ordering in F-actin solutions. *Biophys. J.* 63:794–807.

de Gennes, P.-G. 1990. Introduction to Polymer Dynamics. Cambridge University Press, Cambridge.

De La Cruz, E., and T. D. Pollard. 1994. Transient kinetic analysis of rhodamine phalloidin binding to actin filaments. *Biochemistry*. 33: 14387–14392.

Doi, M. 1975. Rotational relaxation time of rigid rod-like macromolecule in concentrated solution. *J. Physiol. (Paris)*. 36:607–617.

Doi, M., and S. Edwards. 1987. The Theory of Polymer Dynamics. Oxford University Press, Oxford.

Erickson, H. P. 1989. Co-operativity in protein-protein association. *J. Mol. Biol.* 206:465–474.

Frieden, C. 1983. Polymerization of actin: mechanism of the Mg^{2+}-induced process at pH 8 and 20°C. *Proc. Natl. Acad. Sci. USA.* 80: 6513–6517.

Frieden, C., and D. Goddette. 1983. Polymerization of actin and actin-like systems: evaluation of the time course of polymerization in relation to the mechanism. *Biochemistry*. 22:5836–5843.

Furukawa, R., R. Kundra, and M. Fechheimer. 1993. Formation of liquid crystals from actin filaments. *Biochemistry*. 32:12346–12352.

Hitchcock-DeGregori, S. E., P. Sampath, and T. D. Pollard. 1988. Tropomyosin inhibits the rate of actin polymerization by stabilizing actin filaments. *Biochemistry*. 27:9182–9185.

Janmey, P. A., S. Hvidt, J. Käs, D. Lerche, A. Maggs, E. Sackmann, M. Schliwa, and T. P. Stossel. 1994. The mechanical properties of actin gels. *J. Biol. Chem*. 269:32503–32513.

Käs, J., H. Strey, J. X. Tang, D. Finger, R. Ezzell, E. Sackmann, and P. A. Janmey. 1996. F-actin, a model polymer for semiflexible chains in dilute, semidilute, and liquid crystalline solutions. *Biophys. J*. 70: 609–625.

Kaufmann, S., J. Käs, W. H. Goldmann, E. Sackmann, and G. Isenberg. 1992. Talin anchors and nucleates actin filaments at lipid membranes—a direct demonstration. *FEBS Lett*. 314:203–205.

Kawamura, M., and K. Maruyama. 1969. Electron microscopic particle length of F-actin polymerized in vitro. *J. Biochem.* 69:437–457.

Kawamura, M., and K. Maruyama. 1972. A further study of electron microscopic particle length of F-actin polymerized in vitro. *J. Biochem*. 72:179–188.

Kinosian, H. J., L. A. Selden, J. E. Estes, and L. C. Gershman. 1993. Actin filament annealing in the presence of ATP and phalloidin. *Biochemistry.* 32:12353–12357.

Kron, S. J., Y. Y. Toyoshima, T. Q. P. Uyeda, and J. A. Spudich. 1991. Assays for actin sliding movement over myosin-coated surfaces. *Methods Enzymol*. 196:399–416.

Lehrer, S. S. 1972. Crosslinking of actin and of tropomyosin by glutaraldehyde. *Biochem. Biophys. Res. Commun.* 48:967–976.

Lewis, A. K., and P. C. Bridgman. 1992. Nerve growth cone lamellipodia contain two populations of actin filaments that differ in organization and polarity. *J. Cell Biol.* 119:1219–1243.

MacLean-Fletcher, S., and T. D. Pollard. 1980. Identification of a factor in conventional muscle actin preparations which inhibits actin filament self-association. *Biochem. Biophys. Res. Commun.* 96:18–27.

Murphy, D. B., R. O. Gray, W. A. Grasser, and T. D. Pollard. 1988. Direct demonstration of actin filament annealing in vitro. *J. Cell Biol*. 106: 1947–1954.

Oosawa, F., and S. Asakura. 1975. Thermodynamics of the Polymerization of Protein. Academic Press, London, New York.

Pollard, T. D. 1986. Rate constants for the reactions of ATP- and ADP-actin with the ends of actin filaments. *J. Cell Biol.* 103:2747–2754.

Press, W., S. Teukolsky, W. Vetterling, and B. Flannery. 1992. Numerical Recipes in C: The Art of Scientific Computing. Cambridge University Press, Cambridge.

Rickard, J. E., and P. Sheterline. 1988. Effect of ATP removal and inorganic phosphate on length redistribution of sheared actin filament populations: evidence for a mechanism of end-to-end annealing. *J. Mol. Biol.* 201:675–681.

Sampath, P., and T. D. Pollard 1991. Effects of cytochalasin, phalloidin and pH on the elongation of actin filaments. *Biochemistry*. 30: 1973–1980.

Schafer, D., P. Jennings, and J. Cooper. 1996. Dynamics of capping protein and actin assembly in vitro: uncapping barbed ends by polyphosphoinositides. *J. Cell Biol.* 135:169–179.

Suzuki, A., T. Maeda, and T. Ito. 1991. Formation of liquid crystalline phase of actin filament solutions and its dependence on filament length as studied by optical birefringence. *Biophys. J.* 59:25–30.

Tobacman, L. S., and E. D. Korn. 1983. The kinetics of actin nucleation and polymerization. *J. Biol. Chem.* 258:3207–3214.

Warshaw, D. M., J. M. Desrosiers, S. S. Work, and K. M. Trybus. 1990. Smooth muscle myosin cross-bridge interactions modulate actin filament sliding velocity in vitro. *J. Cell Biol.* 111:453–463.

Wegner, A. 1982. Spontaneous fragmentation of actin filaments in physiological conditions. *Nature*. 296:266–267.

Wegner, A., and P. Savko. 1982. Fragmentation of actin filaments. *Biochemistry*. 21:1909–1913.

Xu, J., J. F. Casella, and T. D. Pollard. 1999. Effect of capping protein, CapZ, on the length of actin filaments and mechanical properties of actin filament networks. *Cell Motil. Cytoskeleton*. 42:73–81.